ACSNANO
www.acsnano.org
ARTICLE

Tetracene Formation by On-Surface Reduction

Justus Krüger,[†] Niko Pavliček,[‡] José M. Alonso,[§] Dolores Pérez,[§] Enrique Guitián,[§] Thomas Lehmann,[†] Gianaurelio Cuniberti,[†,∥] André Gourdon,[#] Gerhard Meyer,[‡] Leo Gross,[‡] Francesca Moresco,*[,†] and Diego Peña*[,§]

[†]Institute for Materials Science, Max Bergmann Center of Biomaterials, and Center for Advancing Electronics Dresden, TU Dresden, 01069 Dresden, Germany

[‡]IBM Research—Zurich, 8803 Rüschlikon, Switzerland

[§]Centro de Investigación en Química Biolóxica e Materiais Moleculares (CIQUS) and Departamento de Química Orgánica, Universidade de Santiago de Compostela, Santiago de Compostela 15782, Spain

[#]Centre d'Élaboration de Matériaux et d'Études Structurales (CEMES), UPR 8011 CNRS, Nanosciences Group, 29 Rue Jeanne Marvig, P.O. Box 94347, 31055 Toulouse, France

[∥]Dresden Center for Computational Materials Science (DCMS), TU Dresden, 01069 Dresden, Germany

Supporting Information

ABSTRACT: **We present the on-surface reduction of diepoxytetracenes to form genuine tetracene on Cu(111). The conversion is achieved by scanning tunneling microscopy (STM) tip-induced manipulation as well as thermal activation and is conclusively demonstrated by means of atomic force microscopy (AFM) with atomic resolution. We observe that the metallic surface plays an important role in the deoxygenation and for the planarization after bond cleavage.**

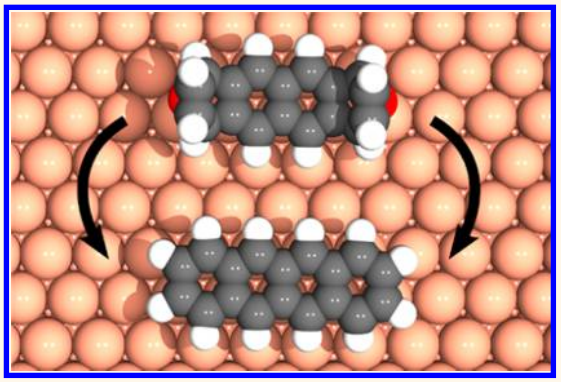

KEYWORDS: *single-molecule chemistry, on-surface reaction, deoxygenation, acenes, atomic force microscopy (AFM)*

The precise fabrication of large acenes and their derivatives offers great promise for application in organic and molecular electronics.[1,2] Their unique electronic properties make them attractive as low bandgap and high mobility materials; however, the synthesis of stable and vacuum- or solution-processable compounds is challenging and becomes even more complex with increasing acene length.[3,4] Therefore, on-surface preparation is an advantageous method which has been proven to be a viable approach in the field of nanoarchitectures,[5−7] *e.g.*, for the fabrication of molecular wires,[8−10] graphene nanoribbons,[11,12] or two-dimensional networks.[13,14] Experimental verification of the underlying synthetic strategies is crucial and relies on high-resolution characterization of the obtained reaction products. Recent advances in atomic force microscopy (AFM) have demonstrated that this method can be well suited to capture surface-assisted formation of acenes due to its powerful capability to image on-surface reaction products in real space. In particular, AFM with atomic resolution has been applied to resolve structures of thermally activated reactions[15−18] and single-molecule chemistry,[19,20] as well as of natural products[21] and mixtures.[22]

RESULTS AND DISCUSSION

In this article, we introduce the on-surface reduction of epoxyacenes to obtain the corresponding acenes, demonstrated by the deoxygenation of a mixture of *syn*/*anti*-**1** to form tetracene (**3**) on Cu(111) as illustrated by Scheme 1. In solution chemistry, this is a nontrivial transformation which requires the use of reducing reagents.[23−27] To explore this

Scheme 1. On-Surface Reduction of Diepoxytetracenes to Form Genuine Tetracene

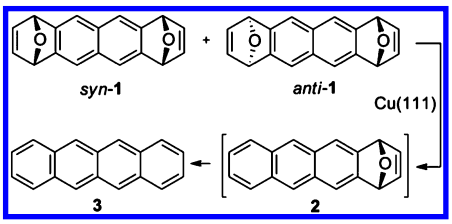

Received: January 22, 2016
Accepted: March 10, 2016

DOI: 10.1021/acsnano.6b00505
ACS Nano XXXX, XXX, XXX−XXX

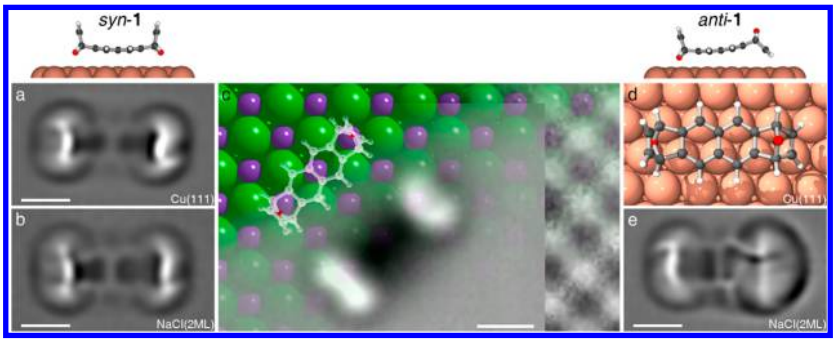

Figure 1. Diepoxytetracenes *syn*/*anti*-1. (a and b) Laplace-filtered AFM images of *syn*-isomer on bare Cu(111) and NaCl (2ML), respectively. (c) Observed adsorption site of a *syn*-isomer on NaCl (2ML). Constant-height AFM measurements with two different tip height domains were employed to resolve the molecular structure as well as the underlying lattice orientation. The experimental gray scale images correspond to the measured unfiltered frequency shift data and features a sharp edge where the tip-height is switched from high to low. In addition, the atomic lattice of NaCl is superimposed to identify the adsorption position. A laterally displaced ball-and-stick model of the free molecule illustrates the close proximity of oxygen atoms and Na atoms of the lattice. (d) Ball-and-stick-model of *anti*-isomer's geometry as calculated for this molecule after full relaxation on a Cu(111) surface. A corresponding experimental AFM image is given in the Supporting Information. (e) Laplace-filtered image of *anti*-isomer on NaCl (2ML) with different contrast on the right-hand side due to protruding oxygen. Unfiltered AFM images are shown in the Supporting Information. All scale bars refer to 5 Å.

reaction on-surface, a mixture of tetracene precursors *syn*/*anti*-**1** was sublimated onto a sample held at below 10 K in ultrahigh vacuum conditions. The used Cu(111) surface featured islands of bilayer NaCl, referred to as NaCl (2ML). In addition, CO molecules were deliberately adsorbed to functionalize the tip.[28] Combined STM and AFM with atomic resolution were employed at a temperature of 5 K to unambiguously characterize the molecular conversion. Moreover, complementary density functional theory (DFT) calculations were performed to determine adsorption geometries of all considered molecules on Cu(111).

Diepoxytetracenes **1** were easily obtained[29] through a double Diels–Alder cycloaddition of a 2,6-naphthodiyne synthon and furan.[30,31] The resulting products **1** are two diastereomers with two 1,4-epoxy groups in either *syn* or *anti* configuration as indicated in Scheme 1. Both molecular species are present on the surface and can be readily imaged by AFM using a CO-functionalized tip, as one can see in the Laplace-filtered images with enhanced contrast in Figure 1. While scanning at constant tip height and due to the nonplanar adsorption geometry, the outer segments of the molecules interact more strongly with the tip and show a less negative frequency shift than the faint contribution of the two inner benzene rings. With decreasing tip height, the strong repulsive (bright) contrast of the outer parts becomes even more pronounced in the raw AFM images (*cf.* Figure S2 in the Supporting Information) before the more closely to the surface adsorbed benzene rings can be fully resolved. Panels a and b of Figure 1 display typical images obtained for *syn*-isomer on bare Cu(111) and NaCl (2ML), respectively, which are characterized by their symmetric shape and reveal additional details at the center due to the applied Laplace-filtering. Apparently, there is no significant difference of the molecular structures on Cu(111) and NaCl (2ML) and the images show that two CH groups are pointing toward the tip on either side of the molecules. Hence, the preferred adsorption geometry coincides with the oxygen-rich side of the molecules facing the surface. This is supported by the determined adsorption site on NaCl (2ML) (see Figure 1c) indicating that electronegative oxygen atoms are located in close proximity to Na atoms. The other possible conformation of a *syn*-isomer with both oxygen pointing away from the surface was not observed in our experiment. On the contrary, adsorbed *anti*-isomers feature always one protruding oxygen atom. This is illustrated by the calculated model in Figure 1d. The resulting Laplace-filtered AFM images are identified by two dissimilar sides as this oxygen atom leads to a clearly different contrast, which is shown in Figure 1e for *anti*-**1** on NaCl (2ML).

To demonstrate the single-molecule conversion reaction, we focused mainly on individual diepoxytetracenes adsorbed onto bare Cu(111). Due to the larger coupling than on NaCl (2ML), the controlled manipulation of such a small molecule proved to be more feasible on the metal.[32] Conformational changes[33] and chemical reactions[34−36] can be induced by applying voltage pulses with the tip of an STM. After characterizing the initial molecule, a chemical conversion was already obtained by constant-current STM imaging with a metal tip at higher bias voltage. The corresponding threshold for any first tip-induced reaction was found to be at ∼2.2 V. A sudden change of the molecular topography while scanning indicated the successful conversion and was confirmed by a subsequent STM scan at low bias of 100 mV. In the case of *syn*-isomer, tetracene generation was usually achieved in a two-step process *via* the formation of epoxytetracene **2** (see an exemplary set of STM images in Figure 2), and both intermediate as well as final reaction product could be characterized by means of constant-height AFM imaging.

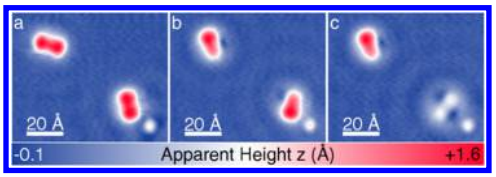

Figure 2. Set of constant-current STM images (V = 100 mV, I = 0.5 pA) acquired with a metal tip to illustrate the stepwise molecular conversion. (a) Two *syn*-isomers 1 on Cu(111) imaged as dumbbell-shaped protrusions. In addition, a defect is visible in the bottom right corner. (b) The resulting intermediate molecules 2 after STM imaging at a voltage of 2.2 V are shown. Faint depressions close to the molecules can be spotted and correspond to cleaved oxygen. (c) Upon application of another higher-voltage scan at V = 2.6 V to the lower molecule, the final conversion to tetracene (3) is obtained.

DOI: 10.1021/acsnano.6b00505
ACS Nano XXXX, XXX, XXX−XXX

Figure 3a,b shows the resulting structure after the first manipulation event (epoxytetracene **2**) and demonstrates that

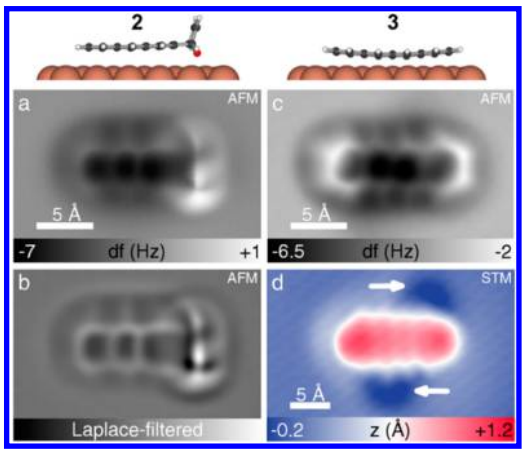

Figure 3. Intermediate 2 and final reaction product 3 after tip-induced conversion of *syn*-isomer on Cu(111). (a and b) Constant-height AFM image and Laplace-filtered data of the intermediate epoxytetracene 2 after the first oxygen detachment. (c) Constant-height AFM image of the resulting tetracene molecule after complete deoxygenation. (d) Constant-current STM image (V = 100 mV, I = 2 pA) of the same molecule. The arrows point to close-by shallow depressions and suggest the presence of atomic oxygen.

one oxygen atom was separated by two C−O bond cleavages. Tip-induced excitation of the molecule is followed by energy dissipation to break bonds and a partial planarization of the remaining molecule will then take place in the presence of a metallic surface. Hence, an additional benzene ring becomes apparent in the AFM image. After the second manipulation step, the molecule was completely planar and an aromatic backbone of four fused benzene rings could be resolved, as indicated in Figure 3c and in accordance to the previously imaged pentacene.[37] In particular, the recorded image shows the same apparent feature that the outer rings are imaged more repulsive than the inner ones. Therefore, the structure of the final reaction product is unambiguously determined to be tetracene (**3**). Further STM images with a CO-terminated tip (*cf.* Figure 3d) reveal that the detached oxygen atoms are situated in close proximity to the newly formed tetracene molecule. They are imaged as indentations which are only observed on the surface after a successful tip-induced reaction.

It is worth noting that using the same manipulation protocol did not lead to the full conversion of *anti*-isomer precursors. After the first successful reduction step, the intermediate molecules **2** were identified to feature the remaining oxygen atom pointing away from the Cu surface. Despite higher voltage scans at up to 3.0 V, the second reduction step was not obtained in the experiment. This suggests that the tip-induced cleavage depends on the orientation of the oxygen with respect to the underlying substrate and a larger O−Cu interaction is favorable for an on-surface reduction. Accordingly, all successful tip-induced reactions were accompanied by a displacement of the molecule, while the separated O atoms remained close to their presumed adsorption site.

To extend this single-molecule reaction to a general preparation method, we investigated also the thermally induced conversion. After annealing of the sample with low coverage (<1% of a monolayer) up to 120 °C for 5 min, the molecules assembled solely at Cu step edges. An exemplary STM overview image is given in the Supporting Information Figure S4. All atomically resolved AFM images (*cf.* Figure 4) showed

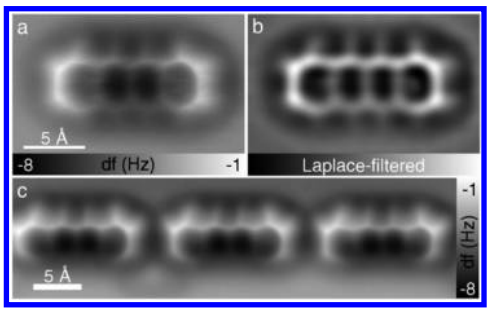

Figure 4. Reaction product 3 on Cu(111) after annealing up to 120 °C. (a and b) AFM and its Laplace-filtered image of an on-surface produced tetracene. (c) AFM image of three tetracene molecules assembled along a step edge. All images were acquired at a constant height.

exclusively the presence of tetracene (**3**) and no diepoxytetracenes **1** were observed. In particular, also no intermediate epoxytetracenes **2** with one oxygen still attached were found in the experiment. This implies that the temperature activated reaction took place at a high rate and regardless of the oxygen orientation of the precursors. However, the latter observation is not necessarily a proof that molecules of *anti*-**1** react in the same way as *syn*-isomers. After the first reduction step, the resulting intermediate **2** may still have considerably different activation barriers to form tetracene depending on the orientation of the remaining oxygen. Upon annealing, molecules diffuse on the surface to more reactive step edges/kink sites or may even switch their oxygen configuration and are then fully reduced due to the enhanced coupling to the Cu; however, the true reaction path remains elusive.

CONCLUSION

In summary, we have demonstrated the on-surface reduction of a diepoxyacene to produce the corresponding acene on Cu(111). Single molecule experiments show a different behavior of *syn* and *anti* diastereoisomeric diepoxyacenes, which suggests that the O−Cu interaction is crucial for the deoxygenation. Notably, thermally induced experiments allow us to prepare tetracene-covered surfaces in a very efficient manner regardless of the starting diastereoisomer. It is clear that the role of the metallic surface is not limited to the deoxygenation but extends to the planarization after bond cleavage. Therefore, the shown reaction leads essentially to the extension of an aromatic system on a metallic surface. Bearing in mind the difficulties associated with the synthesis and manipulation of linear oligoacenes under ambient conditions, low solubility and high reactivity, and the synthetic accessibility to epoxyacenes, this method could pave the way for the access to larger acenes and the development of acene-based molecular devices.

METHODS

Experimental Details. Combined STM/AFM experiments were performed using a home-built instrument operating at a low temperature of $T \approx 5$ K and ultrahigh vacuum ($p \approx 1 \times 10^{-10}$ mbar) conditions. The employed sensor was based on a qPlus design[38] operated in the frequency-modulation mode[39] (eigenfrequency $f_0 \approx$ 31 kHz, quality factor Q on the order of 10^5). All AFM measurements

DOI: 10.1021/acsnano.6b00505
ACS Nano XXXX, XXX, XXX−XXX

were acquired in constant-height mode at V = 0 V and with an oscillation amplitude of $A \approx 0.5$ Å. STM images were taken in constant-current mode with the bias voltage applied to the sample. A Cu(111) single crystal was used as substrate and prepared by repeated cycles of sputtering (Ne^+) and annealing (900 K). After this cleaning procedure, NaCl was evaporated onto the sample at about 270 K in such a way that (100)-oriented NaCl islands of two atomic layer of thickness were formed on the surface. Additionally, CO molecules were deposited with a very low surface coverage and then deliberately picked up by the tip of the STM/AFM to functionalize the apex. The investigated epoxyacenes *syn*/*anti*-**1** were sublimated onto the cold sample ($T \approx 10$ K). Temperature-induced experiments were carried out by transferring the sample out of the STM/AFM to anneal it up to 393 K for 5 min. Subsequently, the sample was cooled again and transferred back inside the STM/AFM without breaking the ultrahigh vacuum at any time.

Computational Details. *Ab initio* density functional theory (DFT) was used to identify the adsorption geometries of all considered molecules on Cu(111). The copper surface was modeled by a periodic slab of five Cu layers, where the three lowest layers were fixed at bulk positions during relaxation. Several initial conditions for the adsorbed molecule obtained from molecular dynamics have been chosen to find the minimum energy configuration. The DFT calculations were performed using a mixed Gaussian and plane wave approach implemented in the Quickstep code of CP2K.[40] Goedecker–Teter–Hutter pseudo potentials[41] with the Perdew–Burke–Ernzerhof exchange-correlation functional[42] and a valence double-ζ basis set was chosen. To correctly account for dispersion effects, we used the nonlocal revised Vydrov–van Voorhies (rVV10) functional.[43] It goes beyond pairwise correction schemes by adding a nonlocal correlation term to the exchange functional, accurately describing the adsorption geometries, in particular the curvature of adsorbed tetracene.

ASSOCIATED CONTENT

Supporting Information

The Supporting Information is available free of charge on the ACS Publications website at DOI: 10.1021/acsnano.6b00505.

Details about synthesis, additional STM/AFM data (PDF)

AUTHOR INFORMATION

Corresponding Authors

*E-mail: francesca.moresco@tu-dresden.de.
*E-mail: diego.pena@usc.es.

Notes

The authors declare no competing financial interest.

ACKNOWLEDGMENTS

We thank R. Allenspach for comments on the manuscript. This work was funded by the ICT-FET European Union Integrated Project PAMS (Agreement No. 610446), the ITN QTea (317485) and the ERC Advanced Grant CEMAS (291194). Support by the German Excellence Initiative *via* the Cluster of Excellence EXC1056 "Center for Advancing Electronics Dresden" (cfaed), the International Helmholtz Research School Nanonet, the DFG and the NSF *via* the common project NSF 11-569, and from the Spanish Ministry of Science and Competitiveness (MINECO, MAT2013-46593-C6-6-P, CTQ2013-44142-P) and FEDER is gratefully acknowledged.

REFERENCES

(1) Anthony, J. E. The Larger Acenes: Versatile Organic Semiconductors. *Angew. Chem., Int. Ed.* **2008**, *47*, 452–83.
(2) Ye, Q.; Chi, C. Recent Highlights and Perspectives on Acene Based Molecules and Materials. *Chem. Mater.* **2014**, *26*, 4046–4056.
(3) Mondal, R.; Shah, B. K.; Neckers, D. C. Photogeneration of Heptacene in a Polymer Matrix. *J. Am. Chem. Soc.* **2006**, *128*, 9612–9613.
(4) Tönshoff, C.; Bettinger, H. F. Photogeneration of Octacene and Nonacene. *Angew. Chem., Int. Ed.* **2010**, *49*, 4125–4128.
(5) Franc, G.; Gourdon, A. Covalent Networks through On-Surface Chemistry in Ultra-High Vacuum: State-of-the-Art and Recent Developments. *Phys. Chem. Chem. Phys.* **2011**, *13*, 14283–92.
(6) Méndez, J.; López, M. F.; Martín-Gago, J. A. On-Surface Synthesis of Cyclic Organic Molecules. *Chem. Soc. Rev.* **2011**, *40*, 4578–4590.
(7) Lindner, R.; Kühnle, A. On-Surface Reactions. *ChemPhysChem* **2015**, *16*, 1582–1592.
(8) Lafferentz, L.; Ample, F.; Yu, H.; Hecht, S.; Joachim, C.; Grill, L. Conductance of a Single Conjugated Polymer as a Continuous Function of Its Length. *Science* **2009**, *323*, 1193–1197.
(9) Gao, H. Y.; Wagner, H.; Zhong, D.; Franke, J. H.; Studer, A.; Fuchs, H. Glaser Coupling at Metal Surfaces. *Angew. Chem., Int. Ed.* **2013**, *52*, 4024–8.
(10) Nacci, C.; Ample, F.; Bleger, D.; Hecht, S.; Joachim, C.; Grill, L. Conductance of a Single Flexible Molecular Wire Composed of Alternating Donor and Acceptor Units. *Nat. Commun.* **2015**, *6*, 7397.
(11) Cai, J.; Ruffieux, P.; Jaafar, R.; Bieri, M.; Braun, T.; Blankenburg, S.; Muoth, M.; Seitsonen, A. P.; Saleh, M.; Feng, X.; Müllen, K.; Fasel, R. Atomically Precise Bottom-up Fabrication of Graphene Nanoribbons. *Nature* **2010**, *466*, 470–3.
(12) Chen, Y.-C.; Cao, T.; Chen, C.; Pedramrazi, Z.; Haberer, D.; de Oteyza, D. G.; Fischer, F. R.; Louie, S. G.; Crommie, M. F. Molecular Bandgap Engineering of Bottom-up Synthesized Graphene Nanoribbon Heterojunctions. *Nat. Nanotechnol.* **2015**, *10*, 156–160.
(13) Grill, L.; Dyer, M.; Lafferentz, L.; Persson, M.; Peters, M. V.; Hecht, S. Nano-Architectures by Covalent Assembly of Molecular Building Blocks. *Nat. Nanotechnol.* **2007**, *2*, 687–91.
(14) Lafferentz, L.; Eberhardt, V.; Dri, C.; Africh, C.; Comelli, G.; Esch, F.; Hecht, S.; Grill, L. Controlling On-Surface Polymerization by Hierarchical and Substrate-Directed Growth. *Nat. Chem.* **2012**, *4*, 215–20.
(15) de Oteyza, D. G.; Gorman, P.; Chen, Y. C.; Wickenburg, S.; Riss, A.; Mowbray, D. J.; Etkin, G.; Pedramrazi, Z.; Tsai, H. Z.; Rubio, A.; Crommie, M. F.; Fischer, F. R. Direct Imaging of Covalent Bond Structure in Single-Molecule Chemical Reactions. *Science* **2013**, *340*, 1434–7.
(16) Riss, A.; Wickenburg, S.; Gorman, P.; Tan, L. Z.; Tsai, H. Z.; de Oteyza, D. G.; Chen, Y. C.; Bradley, A. J.; Ugeda, M. M.; Etkin, G.; Louie, S. G.; Fischer, F. R.; Crommie, M. F. Local Electronic and Chemical Structure of Oligo-Acetylene Derivatives Formed through Radical Cyclizations at a Surface. *Nano Lett.* **2014**, *14*, 2251–5.
(17) Albrecht, F.; Pavliček, N.; Herranz-Lancho, C.; Ruben, M.; Repp, J. Characterization of a Surface Reaction by Means of Atomic Force Microscopy. *J. Am. Chem. Soc.* **2015**, *137*, 7424–7428.
(18) Rogers, C.; Chen, C.; Pedramrazi, Z.; Omrani, A. A.; Tsai, H.-Z.; Jung, H. S.; Lin, S.; Crommie, M. F.; Fischer, F. R. Closing the Nanographene Gap: Surface-Assisted Synthesis of Peripentacene from 6,6′-Bipentacene Precursors. *Angew. Chem., Int. Ed.* **2015**, *54*, 15143–15146.
(19) Mohn, F.; Repp, J.; Gross, L.; Meyer, G.; Dyer, M. S.; Persson, M. Reversible Bond Formation in a Gold-Atom-Organic-Molecule Complex as a Molecular Switch. *Phys. Rev. Lett.* **2010**, *105*, 266102.
(20) Pavliček, N.; Schuler, B.; Collazos, S.; Moll, N.; Pérez, D.; Guitián, E.; Meyer, G.; Peña, D.; Gross, L. On-Surface Generation and Imaging of Arynes by Atomic Force Microscopy. *Nat. Chem.* **2015**, *7*, 623–628.
(21) Gross, L.; Mohn, F.; Moll, N.; Meyer, G.; Ebel, R.; Abdel-Mageed, W. M.; Jaspars, M. Organic Structure Determination Using Atomic-Resolution Scanning Probe Microscopy. *Nat. Chem.* **2010**, *2*, 821–5.
(22) Schuler, B.; Meyer, G.; Peña, D.; Mullins, O. C.; Gross, L. Unraveling the Molecular Structures of Asphaltenes by Atomic Force Microscopy. *J. Am. Chem. Soc.* **2015**, *137*, 9870–9876.

DOI: 10.1021/acsnano.6b00505
ACS Nano XXXX, XXX, XXX–XXX

(23) Chun, D.; Cheng, Y.; Wudl, F. The Most Stable and Fully Characterized Functionalized Heptacene. *Angew. Chem., Int. Ed.* **2008**, *47*, 8380−5.
(24) Eda, S.; Eguchi, F.; Haneda, H.; Hamura, T. A New Synthetic Route to Substituted Tetracenes and Pentacenes Via Stereoselective [4 + 2] Cycloadditions of 1,4-Dihydro-1,4-Epoxynaphthalene and Isobenzofuran. *Chem. Commun.* **2015**, *51*, 5963−6.
(25) Enamorado, M. F.; Ondachi, P. W.; Comins, D. L. A Five-Step Synthesis of (S)-Macrostomine from (S)-Nicotine. *Org. Lett.* **2010**, *12*, 4513−4515.
(26) Ashton, P. R.; Isaacs, N. S.; Kohnke, F. H.; Slawin, A. M. Z.; Spencer, C. M.; Stoddart, J. F.; Williams, D. J. Towards the Making of [12]Collarene. *Angew. Chem., Int. Ed. Engl.* **1988**, *27*, 966−969.
(27) Olah, G. A.; Prakash, G. K. S.; Arvanaghi, M.; Bruce, M. R. Palladium-Catalyzed Reduction of Multiple Bonds with Mg/CH3OH. *Angew. Chem., Int. Ed. Engl.* **1981**, *20*, 92−93.
(28) Mohn, F.; Schuler, B.; Gross, L.; Meyer, G. Different Tips for High-Resolution Atomic Force Microscopy and Scanning Tunneling Microscopy of Single Molecules. *Appl. Phys. Lett.* **2013**, *102*, 073109.
(29) See Supporting Information for details.
(30) Gribble, G. W.; Perni, R. B.; Onan, K. D. Twin Benzannulation of Naphthalene Via 1,3-, 1,6-, and 2,6-Naphthodiyne Synthetic Equivalents. New Syntheses of Triphenylene, Benz[a]Anthracene, and Naphthacene. *J. Org. Chem.* **1985**, *50*, 2934−2939.
(31) Kitamura, C.; Abe, Y.; Ohara, T.; Yoneda, A.; Kawase, T.; Kobayashi, T.; Naito, H.; Komatsu, T. Synthesis and Crystallochromy of 1,4,7,10-Tetraalkyltetracenes: Tuning of Solid-State Optical Properties of Tetracenes by Alkyl Side-Chain Length. *Chem. - Eur. J.* **2010**, *16*, 890−8.
(32) Swart, I.; Sonnleitner, T.; Niedenfuhr, J.; Repp, J. Controlled Lateral Manipulation of Molecules on Insulating Films by STM. *Nano Lett.* **2012**, *12*, 1070−4.
(33) Alemani, M.; Peters, M. V.; Hecht, S.; Rieder, K.-H.; Moresco, F.; Grill, L. Electric Field-Induced Isomerization of Azobenzene by STM. *J. Am. Chem. Soc.* **2006**, *128*, 14446−14447.
(34) Lee, H. J.; Ho, W. Single-Bond Formation and Characterization with a Scanning Tunneling Microscope. *Science* **1999**, *286*, 1719−1722.
(35) Hla, S.-W.; Bartels, L.; Meyer, G.; Rieder, K.-H. Inducing All Steps of a Chemical Reaction with the Scanning Tunneling Microscope Tip: Towards Single Molecule Engineering. *Phys. Rev. Lett.* **2000**, *85*, 2777−2780.
(36) Kumagai, T.; Hanke, F.; Gawinkowski, S.; Sharp, J.; Kotsis, K.; Waluk, J.; Persson, M.; Grill, L. Controlling Intramolecular Hydrogen Transfer in a Porphycene Molecule with Single Atoms or Molecules Located Nearby. *Nat. Chem.* **2014**, *6*, 41−6.
(37) Gross, L.; Mohn, F.; Moll, N.; Liljeroth, P.; Meyer, G. The Chemical Structure of a Molecule Resolved by Atomic Force Microscopy. *Science* **2009**, *325*, 1110−4.
(38) Giessibl, F. J. Atomic Resolution on Si(111)-(7 × 7) by Noncontact Atomic Force Microscopy with a Force Sensor Based on a Quartz Tuning Fork. *Appl. Phys. Lett.* **2000**, *76*, 1470−1472.
(39) Albrecht, T. R.; Grütter, P.; Horne, D.; Rugar, D. Frequency Modulation Detection Using High-Q Cantilevers for Enhanced Force Microscope Sensitivity. *J. Appl. Phys.* **1991**, *69*, 668−673.
(40) VandeVondele, J.; Krack, M.; Mohamed, F.; Parrinello, M.; Chassaing, T.; Hutter, J. Quickstep: Fast and Accurate Density Functional Calculations Using a Mixed Gaussian and Plane Waves Approach. *Comput. Phys. Commun.* **2005**, *167*, 103−128.
(41) Goedecker, S.; Teter, M.; Hutter, J. Separable Dual-Space Gaussian Pseudopotentials. *Phys. Rev. B: Condens. Matter Mater. Phys.* **1996**, *54*, 1703−1710.
(42) Perdew, J. P.; Burke, K.; Ernzerhof, M. Generalized Gradient Approximation Made Simple. *Phys. Rev. Lett.* **1996**, *77*, 3865−3868.
(43) Sabatini, R.; Gorni, T.; de Gironcoli, S. Nonlocal Van Der Waals Density Functional Made Simple and Efficient. *Phys. Rev. B: Condens. Matter Mater. Phys.* **2013**, *87*, 041108.

DOI: 10.1021/acsnano.6b00505
ACS Nano XXXX, XXX, XXX−XXX